

Non-Reciprocity of the Wigner Time Delay in Ballistic Two-Terminal Devices

P. Bredol

Max Planck Institute for Solid State Research, 70569 Stuttgart, Germany

(Dated: September 17, 2020)

In the linear regime, transport properties of ballistic two-terminal devices are generally considered to be independent of the direction of the current. This two-terminal reciprocity applies to both the electron transmission and reflection probabilities. However, it does not apply to the Wigner time delay. Indeed, *four* different time delays describe the transmission and reflection processes from both sides, respectively. Unlike the probabilities, these delays are direction dependent if the channel exchange symmetry of the scattering matrix is broken.

I. INTRODUCTION

Ballistic two-terminal electron devices are known to have reciprocal transport properties in the linear response regime: the transmission of the electrons through these devices is independent of their travel direction. This seems to be obvious, because the transmission and reflection probabilities have to be independent of the direction of the current flow due to the unitarity of the underlying scattering matrix. The functions of existing dissipation-free, two-terminal devices such as capacitors, inductors and tunnel junctions can entirely be understood by means of transmission and reflection probabilities of electrons. Thus, the strict reciprocity of the device properties is guaranteed. However, characterizing a device only by the transmission and reflection probabilities neglects all temporal aspects of the electron transport process. These aspects are captured by the phases of the scattering coefficients, which do not have to be reciprocal.

The Wigner time delay is given by the derivative of the phase of a scattering coefficient with respect to energy and quantifies the duration of the reflection or transmission process of a wave packet interacting with a scatterer¹. For a system with two scattering channels, four time delays exist corresponding to the four entries of the scattering matrix. Three of these four delays can be chosen independently by proper design of the scattering region, which allows non-reciprocal Wigner time delays to be implemented. This contribution focuses on how the device symmetry controls the (non-)reciprocity of the Wigner time delays.

Typical Wigner time delays in optical laboratory setups are on the order of nanoseconds, whereas the delays of electrons traveling through mesoscopic structures are on the order of femtoseconds. The Wigner time delay was measured in photonic systems^{2,3} more than 50 years after the introductory publication of Wigner and Eisenbud¹. Direct measurements of the Wigner time delay of electrons traveling through semiconductor quantum dots were presented first in 2019⁴.

In the following, it is shown that the transmission delays are non-reciprocal in cases where the scattering matrix breaks time-reversal symmetry. The reflection delays are non-reciprocal if the scattering matrix is asymmet-

ric with respect to a simultaneous time reversal and exchange of scattering channels. The non-reciprocity of the Wigner time delay is demonstrated with two analytically solvable examples: an asymmetric potential barrier and an asymmetric Aharonov-Bohm (AB) interferometer⁵. The consequences for both time-dependent and stationary wave functions are presented, and implications for quantum information technology and nanoelectronics are discussed.

II. SYMMETRIES

To determine the symmetry properties of the Wigner time delays of a system, a three dimensional scattering region and two one-dimensional semi-infinite channels are assumed. The position of the scattering region is given by $0 \leq x \leq R$. The first channel extends in negative x direction ($x < 0$), and the second one extends in positive x direction ($x > R$). Outside the scattering region the eigenfunctions $\Phi(\mathbf{r}, k)$ are given by plane waves:

$$\Phi(\mathbf{r}, k) = \begin{cases} (A_1 e^{ikx} + B_1 e^{-ikx}) \cdot \delta(y) \delta(z) & \text{for } x < 0, \\ (A_2 e^{-ikx} + B_2 e^{ikx}) \cdot \delta(y) \delta(z) & \text{for } x > R, \\ \tilde{\Phi}(\mathbf{r}, k) & \text{else,} \end{cases} \quad (1)$$

with the delta distribution δ , $\mathbf{r} = (x, y, z)$, complex amplitudes A_1, A_2, B_1, B_2 and the wave vector k . $\tilde{\Phi}$ denotes the wave function inside the scattering region. The scattering matrix \mathbf{S} transforms the pair of incoming wave amplitudes into the pair of outgoing wave amplitudes $(B_1, B_2)^T = \mathbf{S}(A_1, A_2)^T$ and reads:

$$\mathbf{S} = \begin{pmatrix} s_{11} & s_{12} \\ s_{21} & s_{22} \end{pmatrix} = \begin{pmatrix} \Gamma_{11} e^{i\phi_{11}} & \Gamma_{12} e^{i\phi_{12}} \\ \Gamma_{21} e^{i\phi_{21}} & \Gamma_{22} e^{i\phi_{22}} \end{pmatrix}. \quad (2)$$

To satisfy probability conservation, $\mathbf{S}^\dagger \mathbf{S} = \mathbb{1}$ must hold. This condition requires $\Gamma_{11}^2 + \Gamma_{12}^2 = 1$, $\Gamma_{12} = \Gamma_{21}$ and $\Gamma_{11} = \Gamma_{22} =: \Gamma$. The scattering matrix then reads

$$\mathbf{S} = \begin{pmatrix} \Gamma e^{i\phi_{11}} & \sqrt{1 - \Gamma^2} e^{i\phi_{12}} \\ \sqrt{1 - \Gamma^2} e^{i\phi_{21}} & \Gamma e^{i\phi_{22}} \end{pmatrix}. \quad (3)$$

s_{21} and s_{12} (s_{11} and s_{22}) differ only by a phase factor, the transmission probability from channel 1 to channel 2 ($|s_{21}|^2$) is identical to the transmission probability from channel 2 to channel 1 ($|s_{12}|^2$). The reflection probabilities show an analogous behavior. Thus, all four probabilities are invariant under the exchange of scattering channels, even if the Hamiltonian of the scattering region does not bear this symmetry.

The consequences of this strict reciprocity are remarkable: AB conductance oscillations in two-terminal interferometers are always symmetric with respect to zero magnetic field. Even if the spatial symmetry is broken by the geometry or by applied gate potentials, it is not possible to tune the phase of the oscillation pattern continuously. However, adding further scattering channels removes this so-called phase rigidity, which makes arbitrary oscillation phases possible⁶.

As seen above, the scattering probabilities are fully constrained by the unitarity condition. For the scattering phases ϕ_{ij} , however, unitarity implies only one condition, namely

$$\phi_{11} + \phi_{22} = \phi_{21} + \phi_{12} + \pi. \quad (4)$$

The three remaining degrees of freedom are controlled by two system symmetries: the symmetry with respect to the channel exchange operator \mathcal{P} and to the time-reversal operator \mathcal{T} . Outside the scattering region, the effect of these two operators on the system eigenfunctions as defined in (1) can be understood without knowledge of the scattering region. If \mathcal{P} is applied to an eigenfunction, it simply exchanges A_1 with A_2 and B_1 with B_2 . Applying \mathcal{T} replaces k with $-k$ and conjugates all complex amplitudes A_1 , A_2 , B_1 and B_2 . The effect of the symmetry operations on \mathbf{S} is found by applying the operators to the equation $(B_1, B_2)^T = \mathbf{S}(A_1, A_2)^T$. Applying \mathcal{T} , we obtain

$$\begin{pmatrix} A_1^* \\ A_2^* \end{pmatrix} = \mathcal{T} \mathbf{S} \mathcal{T}^\dagger \begin{pmatrix} B_1^* \\ B_2^* \end{pmatrix}. \quad (5)$$

The time-reversed equation shows that $\mathcal{T} \mathbf{S} \mathcal{T}^\dagger$ is the conjugated inverse matrix $(\mathbf{S}^{-1})^*$. Owing to $\mathbf{S}^{-1} = \mathbf{S}^\dagger$, applying \mathcal{T} to \mathbf{S} is equivalent to transposing \mathbf{S} . Applying \mathcal{P} to $(B_1, B_2)^T = \mathbf{S}(A_1, A_2)^T$, we obtain

$$\begin{pmatrix} B_2 \\ B_1 \end{pmatrix} = \mathcal{P} \mathbf{S} \mathcal{P}^\dagger \begin{pmatrix} A_2 \\ A_1 \end{pmatrix}. \quad (6)$$

The channel exchange transposes \mathbf{S} and exchanges the diagonal elements. Thus, the combined operation $\mathcal{P}\mathcal{T}$ exchanges only the diagonal elements of s_{11} and s_{22} . The following relations hold for the phases of the scattering coefficients:

$$\mathbf{S} = \mathcal{P} \mathbf{S} \mathcal{P}^\dagger \quad \Leftrightarrow \quad \phi_{11} = \phi_{22} \text{ and } \phi_{12} = \phi_{21}, \quad (7)$$

$$\mathbf{S} = \mathcal{T} \mathbf{S} \mathcal{T}^\dagger \quad \Leftrightarrow \quad \phi_{12} = \phi_{21}, \quad (8)$$

$$\mathbf{S} = \mathcal{P}\mathcal{T} \mathbf{S} \mathcal{T}^\dagger \mathcal{P}^\dagger \quad \Leftrightarrow \quad \phi_{11} = \phi_{22}. \quad (9)$$

If (7) holds, full reciprocity follows. If (7) is broken, but (8) holds, (9) is broken as well. Consequently, the transmission phases are reciprocal but the reflection phases are not. Vice versa, if (7) and (8) are broken, but (9) holds, the reflection phases are reciprocal but the transmission phases are not.

In the following, two analytically solvable example systems are presented, each of which fulfills one of the symmetries (8) or (9), but break the other one. The results are obtained by solving the one-dimensional Schrödinger equation for a free particle with mass m and charge q in presence of an electromagnetic vector potential \mathbf{A} . In natural units $\hbar = q = 2m = 1$, the Hamiltonian reads

$$\mathbf{H} = (-i\partial_x - \mathbf{A})^2. \quad (10)$$

The potential barrier shown in Fig. 1 is time-reversal symmetric but not invariant under channel exchange. It fulfills (8) but breaks (9). Figure 1b shows the resulting scattering coefficients as a function of energy. As expected, both transmission coefficients are identical and the reflection coefficients differ by a phase factor. For energies much lower than the barrier height, the transmission probability vanishes, whereas for energies much higher than the barrier height, transparency is approached. As dictated by unitarity, the transmission and reflection probabilities are identical for forward and reverse direction.

The asymmetric AB interferometer shown in Fig. 2 consists of four one-dimensional waveguides connected by two beam splitters. The eigenfunctions in the waveguides are described by plane waves, and the two beam splitters are characterized by the energy-independent three-channel scattering matrix

$$\mathbf{S}_{BS} = \begin{pmatrix} 0 & \frac{1}{\sqrt{2}} & \frac{1}{\sqrt{2}} \\ \frac{1}{\sqrt{2}} & -\frac{1}{2} & \frac{1}{2} \\ \frac{1}{\sqrt{2}} & \frac{1}{2} & -\frac{1}{2} \end{pmatrix}. \quad (11)$$

As depicted in Fig. 2, channel 1 of each beam splitter is connected to one of the infinite waveguides leaving to the left and right. Channels 2 and 3 of the beam splitters are connected to the lower and upper interferometer arm, respectively. The asymmetric AB interferometer is neither time-reversal symmetric nor symmetric with respect to channel exchange. Both symmetry operations are equivalent to the reversal of the enclosed magnetic flux. Thus, the combined operation $\mathcal{P}\mathcal{T}$ leaves the system unchanged, and the interferometer fulfills (9) but breaks (8). As Fig. 2b confirms, both reflection coefficients are identical, and the transmission coefficients differ by a phase factor. The transmission and reflection probabilities show numerous resonances due to the energy dependence of the phase difference acquired between the two arms

$$\Delta\phi = \Delta lk \pm 2\pi\Phi/\Phi_0, \quad (12)$$

with the magnetic flux quantum $\Phi_0 = h/e = 2\pi$ in the chosen natural units. The plus and minus sign correspond to the $1 \rightarrow 2$ and $2 \rightarrow 1$ directions, respectively.

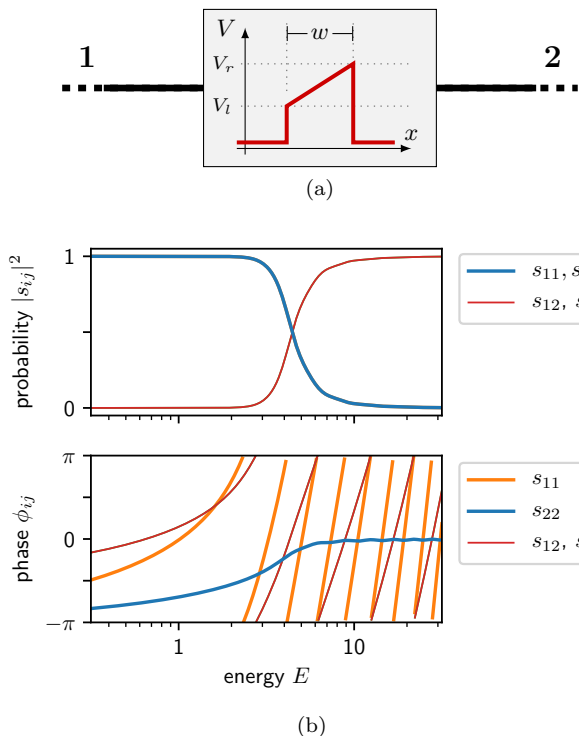


Figure 1. (a) Asymmetric potential barrier embedded in an infinite waveguide. Scattering channel 1 and 2 correspond to the waveguide leaving to the left and right, respectively. The potential is characterized by its width w , the left side potential height V_l and the right side potential height V_r . (b) Polar representation of the scattering coefficients calculated as a function of energy for $w = 5$, $V_l = 0$ and $V_r = 5$ in natural units $\hbar = q = 2m = 1$.

If the phase difference $\Delta\phi$ is a multiple of 2π and with \mathbf{S}_{BS} as defined above, full transparency follows. Using $\Phi_0 = 2\pi$, $E = k^2$ and the system parameters $\Delta l = \frac{\pi}{4}$ and $\Phi = \frac{\pi}{2}$, equation (12) shows that transparency is achieved for $E = 4$. In all other cases, the behavior cannot be easily understood by tracing individual paths and their accumulated phase differences $\Delta\phi$ because many partial reflections at the beam splitters and a large number of round trips in the interferometer may occur along the paths.

III. NON-RECIPROCALITY OF THE WIGNER TIME DELAY

After the previous section demonstrated the effects of the system symmetries on the scattering coefficients and their non-reciprocal phases, in this section the resulting non-reciprocal Wigner time delays are presented. The Wigner time delay was introduced by Wigner and Eisenbud in 1947¹ and is defined as the derivative of the scattering phase with respect to energy,

$$\tau_{ij} = \hbar \frac{\partial \phi_{ij}}{\partial E}. \quad (13)$$

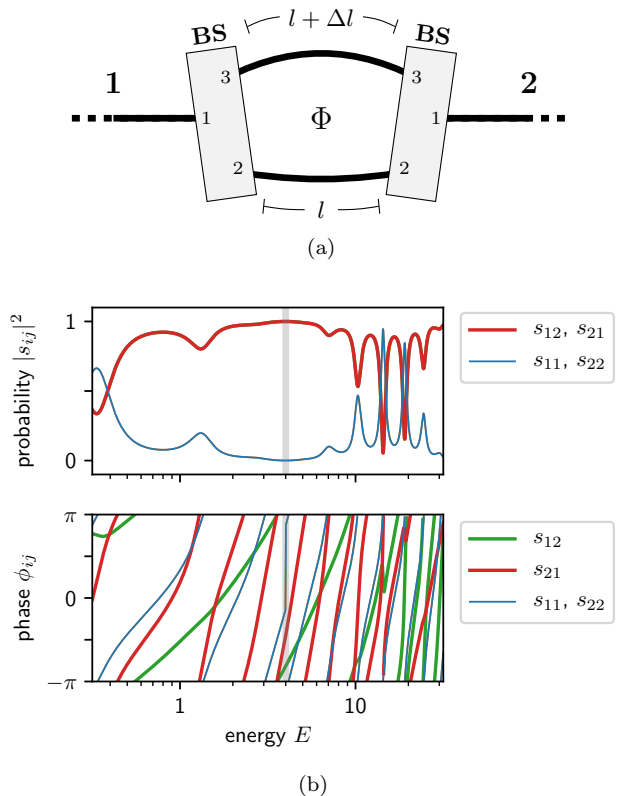


Figure 2. (a) Asymmetric AB interferometer composed of four waveguides (black lines) and two beam splitters (gray boxes). The small numbers 1–3 denote the respective channel indices of the beam splitter scattering matrix \mathbf{S}_{BS} . The composed system has two channels (bold numbers), which correspond to the waveguides leaving to the left and right, respectively. The interferometer is characterized by the enclosed magnetic flux Φ and the arm lengths l and $l + \Delta l$. (b) Polar representation of the scattering coefficients calculated as a function of energy for $l = 5$, $\Delta l = \frac{\pi}{4}$ and $\Phi = \frac{\pi}{2}$ in natural units $\hbar = q = 2m = 1$. Transparency is achieved for $E = 4$ (gray line). The phase jump of π in the reflection phase is in accordance with the corresponding zero in the reflection probability.

To understand this definition, it is instructive to study the undisturbed motion of a Gaussian wave packet first. According to the Hamiltonian (10), the temporal evolution of such a wave packet in an infinite one-dimensional waveguide reads

$$\psi(k, t) = A \exp \left(-\frac{(k - k_0)^2}{2\sigma^2} - ik[x_0 + kt] \right), \quad (14)$$

where $k = \pm\sqrt{E}$ is the momentum. The wave packet is centered around k_0 with width σ in momentum space; in position space it is centered at $x_0 + kt$. A is the normalization constant. After transmission or reflection, as described by one of the coefficients $s_{ij} = \Gamma_{ij} e^{i\phi_{ij}}$, the wave

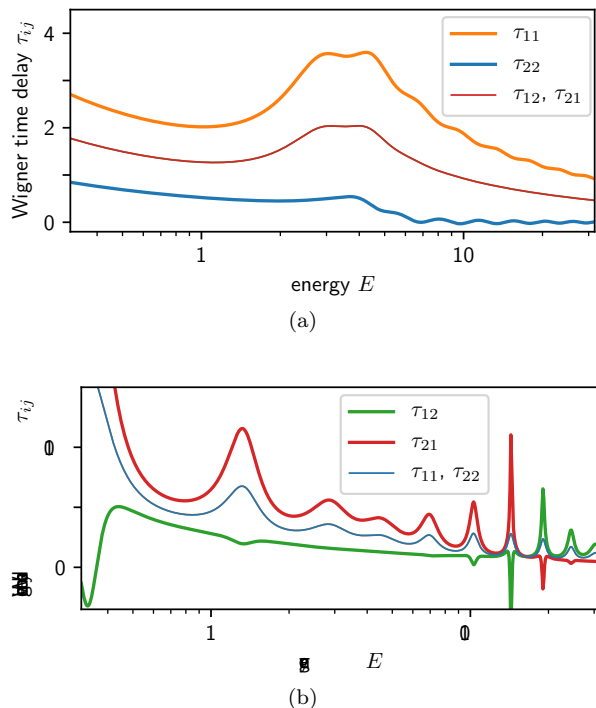


Figure 3. (a) Wigner time delays of the asymmetric potential barrier introduced in Fig. 1. Reflection delays are generally different in forward and reverse direction. (b) Respective plot for the asymmetric AB interferometer introduced in Fig. 2. For this system, the transmission delays are non-reciprocal.

function is given by

$$s_{ij}(k)\psi(k, t) = \Gamma_{ij}(k) \cdot A \exp \left(-\frac{(k - k_0)^2}{2\sigma^2} - ik \left[x_0 + k \left(t - \frac{\phi_{ij}(k)}{k^2} \right) \right] \right). \quad (15)$$

The term proportional to k^2 in ϕ_{ij} plays the role of a time delay in the motion of the wave packet's center. Owing to the quadratic dispersion $E = k^2$, this term corresponds to the first order of the derivative of ϕ_{ij} with respect to energy. Figure 3 shows the four resulting delays as a function of energy for the two systems introduced in the previous section.

For wave packets, only the scattering phases in a certain energy window are relevant. If the packet is narrow in momentum space, this window is small and the scattering phases are linear in energy to a good approximation. τ_{ij} is then energy-independent in the relevant range. For wider wave packets, the energy dependence of the delay deforms the wave packet in addition to the broadening following from the standard $E = k^2$ dispersion.

The Wigner time delay and its role in quantum transport have been extensively discussed⁷. The literature also reports numerous non-reciprocal electron transport phenomena⁸. Non-reciprocal wave packet dynamics was shown earlier in^{5,9}. Here, the analytic solution of the

continuous Schrödinger equation and the Wigner time delay as a quantitative measure of the wave packet dynamics is presented. Closely related subjects are the violation of Onsager's (magnetic field) symmetry in wave packet transport^{10,11} and the optical effect called directional birefringence, which features a velocity that depends on the direction of propagation¹².

Both the asymmetric potential barrier and the asymmetric AB interferometer are characterized by non-reciprocal Wigner time delays (Fig. 3). A direct way to visualize the Wigner time delay is to study the time evolution of wave packets. Figure 4a shows how the deviating Wigner time delays $\tau_{11} \neq \tau_{22}$ of the asymmetric potential barrier (Fig. 1) affect the scattering dynamics of wave packets. A wave packet traveling towards the system from channel 2 is reflected quickly and the time spent in the scattering region is short ($3 < t < 5$). The mirrored wave packet approaching from channel 1 spends a longer time inside the scattering region ($3 < t < 8$) before ejection. The transmitted wave function is identical for both cases. Figure 4b shows the respective situation with the asymmetric AB interferometer (Fig. 2), where $\tau_{21} \neq \tau_{12}$. The wave packet is transmitted quickly if it approaches from channel 2. The time spent in the scattering region is short ($2.5 < t < 7$).

In the case where it approaches from channel 1, the wave packet experiences reflections at the beam splitters and spends a longer time ($2.5 < t < 10$) in the interferometer⁵. Almost no reflection occurs because the transmission probability is exactly 1 at $k_0 = \pm 2$ and close to unity in the vicinity of k_0 .

The time evolution of wave packets is the most direct way to access the Wigner time delay, but its validity is not limited to time-dependent wave functions. It is also reflected in the probability amplitude of eigenfunctions inside the scattering region. The relation between Wigner time delay and eigenfunction amplitude can be understood easily by taking a closer look at eigenfunctions of the asymmetric AB interferometer (Fig. 2a). At $E = 4$, where the device is transparent, the eigenfunction with a plane wave entering only from channel 2 ("fast" direction) consists of left-moving plane waves *only*. The respective eigenfunction with plane waves entering only from channel 1 ("slow" direction) consists of right-moving *and* left-moving plane waves in the interferometer arms. The presence of both plane wave directions in the interferometer arms is necessary for the additional round trip⁵ that the wave packet takes in the interferometer in the "slow" direction. To be able to travel back and forth, the eigenstates making up the wave packet must contain plane waves of both propagation directions. In the "fast" direction, the wave packet traverses the interferometer smoothly without internal reflections. Therefore the respective eigenstates consist only of plane waves moving in one direction.

This reasoning generalizes to any energy: The eigenfunctions injecting plane waves in the "fast" direction consist predominantly of plane waves moving in the same

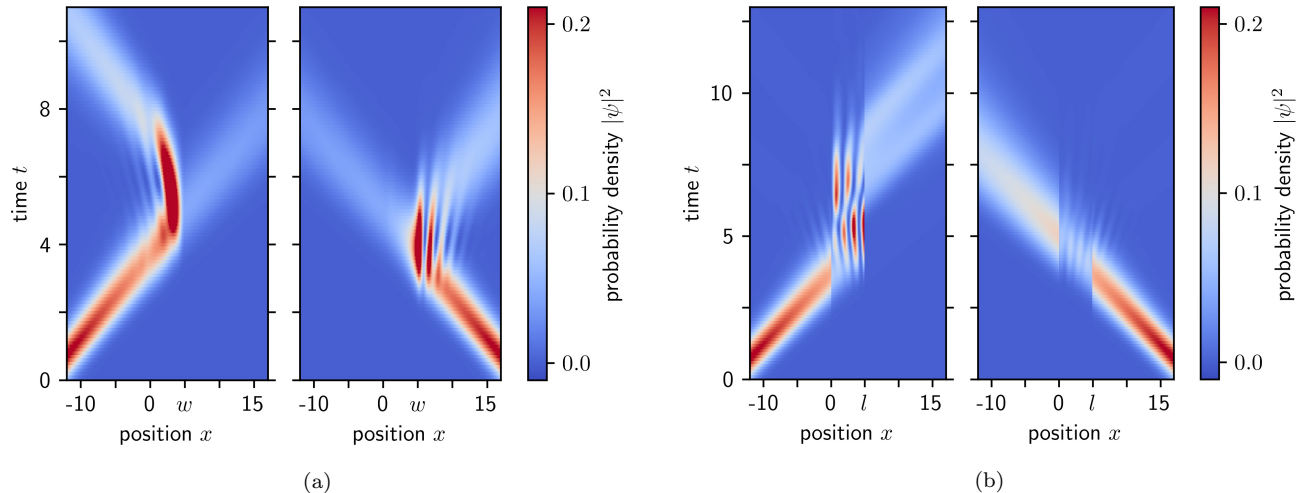


Figure 4. (a) Time-resolved scattering of a wave packet by the asymmetric potential barrier introduced in Fig. 1. In the left (right) plot, the wave packet is injected from channel 1 (2). The wave packet’s central momentum is $k_0 = \pm 2$, the momentum spread is $\sigma = 0.4$. The packet position at $t = 0$ is $x_0^L = -15$ in channel 1 and $x_0^R = -x_0^L + w = -x_0^L + l = 20$ in channel 2. (b) Respective plot for the asymmetric AB interferometer introduced in Fig. 2. In the range $0 < x < l$, only the probability density of the wave function in the lower interferometer arm is shown. The wave packet parameters are equal to those used in (a).

direction in the interferometer arms. Eigenfunctions that inject plane waves in the “slow” direction contain more counter-moving plane waves in the interferometer arms. Naturally, these additional plane waves contribute to the probability amplitude within the scattering region. We therefore expect the local probability amplitude n , defined as

$$n(E) = \int_0^R dx \int_{-\infty}^{\infty} dy \int_{-\infty}^{\infty} dz |\Phi(x, y, z)|^2, \quad (16)$$

to be associated with the Wigner time delay. The eigenfunctions Φ are normalized such that the incoming wave has an amplitude of 1. Figure 5 shows $n(E)$ for both example systems and confirms the expected similarity with the Wigner time delay. The direction with the longer Wigner time delay τ_{ij} also has a higher n . A peculiarity of this relation is that τ_{ij} is defined in equation (13) as a derivative with respect to E , thus by all states around a fixed E . However, n is a property of the unique state belonging to E .

IV. DISCUSSION

These two prototypical example systems demonstrate that the Wigner time delay is less constrained by the unitarity condition than the transmission and reflection probabilities. Hence, symmetries that are required for these probabilities are not obligatory for the Wigner time delay. In particular, reflection and transmission delays may be non-reciprocal in two-terminal devices. In quantum information technology, the direction-dependent delay of wave packets is relevant for the routing and process-

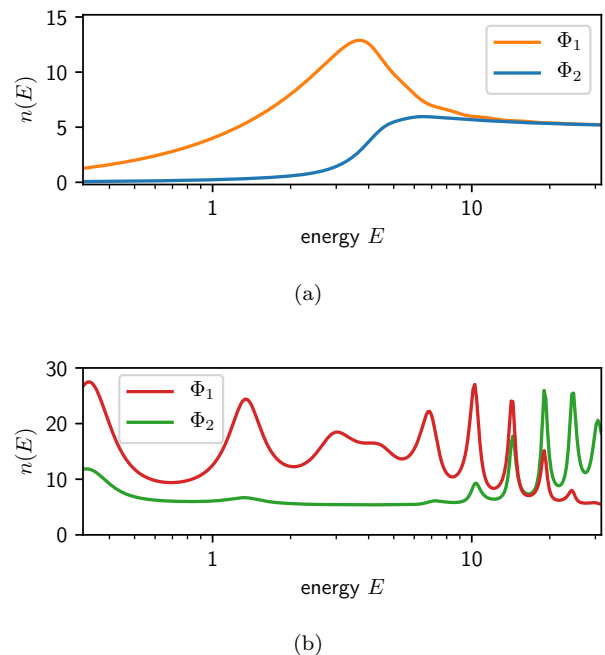


Figure 5. (a) Non-reciprocal local probability amplitude n of eigenfunctions of the asymmetric potential barrier introduced in Fig. 1. Φ_1 refers to eigenfunctions with an incoming plane wave from channel 1 but no incoming wave from channel 2, Φ_2 refers to eigenfunctions with incoming plane waves only from channel 2, not from channel 1. A comparison with Fig. 3 confirms that longer Wigner time delays lead to higher amplitudes of the wave function inside the scattering region. (b) Respective plot for the asymmetric AB interferometer introduced in Fig. 2.

ing of flying qubits¹³. In mesoscopic electronic devices, the Wigner time delay leads to an additional quantum capacitance^{14,15}. In both cases, the non-reciprocity presented here has not been considered so far.

Is it possible to violate the two-terminal conductance reciprocity if the non-reciprocal delays are combined with inelastic scattering or interaction effects? The longer Wigner time delay leads to a higher probability for inelastic interaction with defects localized in the scattering region and therefore affects the conductivity. Thus, in such cases, non-reciprocal Wigner time delays may lead to non-reciprocal two-terminal conductance^{5,9,16}. Analyzing the properties of buckled silicene AB rings, Szafran *et al.* have shown that inter-valley scattering converts oscillations of the Wigner time delay into conductance oscillations¹⁷.

V. CONCLUSIONS

The Wigner time delay is an important characteristic of the dynamics in quantum transport and is thus of fundamental and technological importance^{9,13–15}. The two-channel case plays a special role because energy conservation dictates reciprocal scattering probabilities. This reciprocity cannot be broken by means of asymmetry of the system. The Wigner time delay, however, is non-

reciprocal in two situations:

1. If the scattering matrix breaks time-reversal symmetry, non-reciprocity of the transmission delays follows.
2. If the scattering matrix is asymmetric with respect to a simultaneous reversal of time and exchange of scattering channels, the reflection delays are non-reciprocal.

Furthermore, the Wigner time delay is associated with properties of individual eigenstates: The longer the delay, the higher the local probability amplitude of the eigenstate in the scattering region. The non-reciprocity of the Wigner time delay may lead to novel quantum gates for flying qubits. The interplay with decoherence caused by inelastic scattering may make it possible to violate the otherwise strictly required two-terminal conductance reciprocity.

ACKNOWLEDGMENTS

The author thanks J. Mannhart for pointing out the direction-dependent local probability amplitude and gratefully acknowledges useful discussions with him, H. Boschker, D. Braak and D. Manske and support by L. Pavka.

-
- ¹ E. P. Wigner and L. Eisenbud, Higher angular momenta and long range interaction in resonance reactions, *Phys. Rev.* **72**, 29 (1947).
 - ² D. Chauvat, O. Emile, F. Bretenaker, and A. Le Floch, Direct measurement of the wigner delay associated with the goos-hänchen effect, *Phys. Rev. Lett.* **84**, 71 (2000).
 - ³ R. Bourgain, J. Pellegrino, S. Jennewein, Y. R. P. Sortais, and A. Browaeys, Direct measurement of the wigner time delay for the scattering of light by a single atom, *Opt. Lett.* **38**, 1963 (2013).
 - ⁴ G. Yamahata, S. Ryu, N. Johnson, H.-S. Sim, A. Fujiwara, and M. Kataoka, Picosecond coherent electron motion in a silicon single-electron source, *Nat. Nanotechnol.* **14**, 1019 (2019).
 - ⁵ J. Mannhart, Non-reciprocal interferometers for matter waves, *J. Supercond. Nov. Magn.* **31**, 1649 (2018).
 - ⁶ S. S. Buchholz, S. F. Fischer, U. Kunze, M. Bell, D. Reuter, and A. D. Wieck, Control of the transmission phase in an asymmetric four-terminal aharonov-bohm interferometer, *Phys. Rev. B* **82**, 045432 (2010).
 - ⁷ C. Texier, Wigner time delay and related concepts: Application to transport in coherent conductors, *Physica E: Low Dimens. Syst. Nanostruct.* **82**, 16 (2016).
 - ⁸ Y. Tokura and N. Nagaosa, Nonreciprocal responses from non-centrosymmetric quantum materials, *Nat. Commun.* **9** (2018).
 - ⁹ P. Bredol, H. Boschker, D. Braak, and J. Mannhart, Quantum collapses break reciprocity in matter transport, preprint (2019), arXiv:1912.11948 [cond-mat.mes-hall].
 - ¹⁰ R. Kalina, B. Szafran, S. Bednarek, and F. M. Peeters, Magnetic-field asymmetry of electron wave packet transmission in bent channels capacitively coupled to a metal gate, *Phys. Rev. Lett.* **102**, 066807 (2009).
 - ¹¹ B. Szafran, M. R. Poniedzialek, and F. M. Peeters, Violation of onsager symmetry for a ballistic channel coulomb coupled to a quantum ring, *EPL* **87**, 47002 (2009).
 - ¹² A. M. Kuzmenko, V. Dziom, A. Shuvaev, A. Pimenov, M. Schiebl, A. A. Mukhin, V. Y. Ivanov, I. A. Gudim, L. N. Bezmaternykh, and A. Pimenov, Large directional optical anisotropy in multiferroic ferroborate, *Phys. Rev. B* **92**, 184409 (2015).
 - ¹³ M. Yamamoto, S. Takada, C. Bäuerle, K. Watanabe, A. D. Wieck, and S. Tarucha, Electrical control of a solid-state flying qubit, *Nat. Nanotechnol.* **7**, 247 (2012).
 - ¹⁴ Z. Ringel, Y. Imry, and O. Entin-Wohlman, Delayed currents and interaction effects in mesoscopic capacitors, *Phys. Rev. B* **78**, 165304 (2008).
 - ¹⁵ M. Büttiker, Time-dependent transport in mesoscopic structures, *J. of Low Temp. Phys* **118**, 519 (2000).
 - ¹⁶ J. Mannhart, P. Bredol, and D. Braak, Phase filters for a novel kind of asymmetric transport – scientific prospects and opportunities for possible applications, *Physica E: Low Dimens. Syst. Nanostruct.* **109**, 198 (2019).
 - ¹⁷ B. Szafran, B. Rzesotarski, and A. Mreńca-Kolasińska, Topologically protected wave packets and quantum rings in silicene, *Phys. Rev. B* **100**, 085306 (2019).